Chacterization of a 20 kHz sonoreactor: Part I: Analysis of mechanical effects by classical and numerical methods

V. Sáez[a], A. Frías-Ferrer[a], J. Iniesta[a], J. González-García[a1], A. Aldaz[a] y E. Riera[b]
[a]*Grupo de Electroquímica Aplicada y Electrocatálisis, Departamento de Química Física. Universidad de Alicante. Ap. Correos 99. 03080 Alicante (Spain).*
[b]*Instituto de Acústica, CSIC, Serrano 114, 28006 Madrid (Spain)*

Keywords: sonoreactor, ultrasonic intensity, characterization, thermal probe, aluminium test

Abstract

Numerical simultations have been carried out in order to characterize the ultrasonic field propagation and to obtain the spatial distribution of the mechanical effect derived from it. The results have been compared with those obtained with different classical physical methods (calorimetry, aluminium foil erosion, thermal probes) and have given useful information about the influence of the presence of probes and auxiliary tools in the ultrasonic field. All these information have been used for the development of the Part II of this work: analysis of chemical effects, providing an accurate picture of the reaction environment in the sonoreactor used (20kHz, 100W supplied by Undatim) for further uses in sonoelectrochemical studies.

1. Introduction

The ultrasound science and technology are becoming a growing research field [1] because of a wide range of emerging applications in chemical synthesis, therapeutics, environmental protection, electrochemistry, proceesing of food, processing of solids and liquids [2]. However, it has been stressed in literature the difficulty of the development of the scale-up strategies from laboratory to industrial scale [3,4],

[1] Corresponding author: jose.gonzalez@ua.es

particularly in the sonoreactor design. Several causes have been highlighted [5,6], such as: (i) marked effects localized near the surface of the sonicator (ii) non-uniform and non-optimized volumetric energy density (iii) erosion of the sonic horn surface at high power intensities and (iv) a perfectible transducer technology. At this stage, it is very important to characterize the behaviour of sonoreactors in order to identify accurately the actives zones, especially those related to the cavitation events, as well as it might also shed light on an accurate picture on the reaction environment in the sonoreactor.

On the other hand, attention is being paid on the subdivision of the sonochemical applications based on the "true" and "false" effects [7]: Several differences are established between the chemical effects (resulting from the cavitation event) and the effects caused by the mechanical actions (mainly as a consequence of the bubble collapse) Regarding the above subdivision, we can find in the literature a large number of methods, and also classifications of them [8,9], which characterize the sonoreactor behaviour. These analyses have been devised to measure the effects of ultrasound [10,11], especially the ultrasonic power, but recently there is a increasing number of papers studying the mechanical effects [12-25] including modelling techniques [26-31].

Classical methods designed for mechanical effect studies use hydrophones [5,6], aluminium foil erosion [12-14] and thermistors and thermoelectrical probes [15-19] for local measurements and the calorimetric method [20-25] for global measurements.

In the present work the sonoreactor® Undatim 20kHz/100W has been chacarterizated with numerical simulation and the results have been compared with those obtained with several mostly used classical methods.

2. Experimental

2.1. Equipments

The sonoreactor was a jacketed Sonoreactor® (20 kHz, 100 W maximum power, 68 mm diameter, 84 mm depth) supplied by Undatim. This apparatus can operate at optimum frequency by means of an electronic device and so ensure a maximum power transmitted to the reactor. A sketch of the experimental cell is shown in figure 1. The sonicated volume (200 mL for each experiment) presented a cylindrical tall shape with 68 mm of diameter and 41 mm of height. Temperature was measured and monitored for the calorimetric experiments with a thermistor (Pt100 Thermometer 638 Pt, Crison) and with a thermocouple (JMTSS-020G-6, OMEGA) for the thermal distribution experiments. A titanium stepped horn (7.07 cm^2 emitter area) was used as ultrasound source and was fitted at the bottom of the cell.

2.2 Classical physical methods

Several classical methods were used to obtain a general characterization. In order to determinate the dissipated power (global ultrasonic intensity) into the system calorimetric method with water was used [20-25]. The aluminium foil analysis [12-14] was used to detect the mechanical effects coming from the cavitation events. Thermal distribution analysis was obtained using the technique presented by Romdhane et al. [18].

2.3 Numerical Simulations

Numerical simulations have been carried out in order to study the ultrasonic field propagation. To do that, linear wave propagation in an homogeneous media have been assumed as so they can be described with the wave equation

$$\nabla\left(\frac{1}{\rho}\nabla P\right)-\frac{1}{\rho c^2}\frac{\partial^2 P}{\partial t^2}=0 \qquad (1)$$

where P is the acoustic pressure, ρ is the density and c is the speed of the sound. The transducer system used in ultrasound works at certain frequency so it is common to consider one case when pressure P is time harmonic. In time harmonic case

$$P(r,t)=p(r)e^{i\omega t} \qquad (2)$$

where the spatial variable r = r(x, y, z) and ω is the angular frequency. The space dependent part of the pressure is the solution of the Helmholtz equation

$$\nabla\left(\frac{1}{\rho}\nabla p\right)+\frac{\kappa^2}{\rho}p=0 \qquad (3)$$

where κ is the wavenumber (κ = 2πf/c) and f is the frequency of the field. The limitations of the Helmholtz model are it does not take into account nonlinear wave propagation and the generation of transversal elastic waves (shear waves).

With suitable boundary conditions the Helmholtz equation (3) can be solved using a variety of numerical methods. The standard approaches include low-order finite element method [32-34] and finite difference method.

On the other hand, the quality of the numerical solution of the Helmholtz equation depends significantly on the wavenumber, κ. The solution at a high wavenumber κ is highly oscillatory. Consequently, the discretization stepsize h of a

numerical method has to be sufficiently refined to solve the oscillations. A typical rule for such an adjustment is to force [33,35,36]

$$\kappa \cdot h = \text{constant} \qquad (4)$$

which implies the unchanged resolution, i.e. the same grid points (or elements) per wavelength used. However, it is known [33] that, for κh=constant, the errors of the finite element solutions deteriorate rapidly as the wavenumber κ increases. This non-robust behaviour with respect to κ is known as the pollution effect [36-42]. The pollution effect may be reduced by increasing the order of the elements in the finite element method or using a small enough mesh for the resolution. In this present work the second choice has been chosen and a small enough mesh for the resolution of the system has been used.

Finally, the boundary conditions used were pressure, p = 0 at the upper boundary edge where water is in contact with atmosphere, where p is the pressure, $\delta p/\delta n=0$ at the walls, where n is a normal vector to the boundary surface, and $p=p_0$ at the emitter surface, where p_0 is the amplitude of the wave.

Commercial finite element software package FEMLAB 3.0 has been used to solve the Helmholtz equation.

3. Results

3.1 Classical physical methods

Figure 2 shows the aluminium foil analysis (effect of the distance and ultrasonic intensity) and figure 3 shows the profiles for the thermal intensity at different global ultrasonic intensities. From the results obtained from the classical physical methods, a general picture of the ultrasonic field can be drawn as follows: the mechanical effects are located close to the emitter centre, inside a circumference of 40 mm diameter. The most important information is located around the axial direction, with a modular distribution of the active zones, supported by the thermal distribution analysis from figure 3. This distribution changes from a spindle like shape at lower global ultrasonic intensities (3.39 W cm^{-2}) to a thin-cylinder like shape at higher global ultrasonic intensities (7.64 W cm^{-2}). All these results are in agreement with other reported in literature [43].

3.2 Numerical Simulations results

Several features have been analysed using this method. Figures 4 show the calculated spatial variations in the acoustic pressure amplitude, in water, as a function of the distance from the emitter (circular plane piston) in the axial (coordinate Y) and the radial (coordinate X) directions for (a) 1.84 and (b) 7.64 W cm^{-2}. Similarly, Figure 5 shows the variation of pressure in the centre of the transducer along the axial direction for the ultrasonic intensities range studied. These results agree with those obtained from the classical methods without variations detected close to cell walls and a gradual variation in the pressure, with negative pressures associated to the cavitation events.

Keeping in mind the final use of this sonoreactor for sonoelectrochemical studies, the pressure mapping has been analyzed at 5.09 W cm^{-2} for different configurations. Thus, Figure 6a shows the great influence of the implementation of the

glass cooling coil (see experimental section), modifying the ultrasonic field. Similar results have been obtained for the other global ultrasonic intensities and so, figure 6b shows the variation of the pressure with the distance from the emitter surface for them only in the axial direction at X=0. It is very important to emphasis the modification of the node position and the higher values for the negative pressures at distances higher than 2.5 cm from the emitter surface thereby, assisting the cavitation events.

On the other hand, the incorporation of a rod shaped probe does not vary notoriously the field as shown in Figure 7 for any global ultrasonic intensity or distance. This result is very interesting in order to carry out sonoelectrochemical experiments because the immersed working electrode will not modify the ultrasonic field during the measurement.

4. Conclusions

The main objective of the present work accomplishes the validation of numerical simulations as an analysis technique to characterize the ultrasound field propagation. Similar pictures are obtained with both approaches used in this work (classical and numerical methods) and consequently, from these results, the use of this kind of numerical simulation is a promising tool for prediction of the behaviour of new configurations.

On the other hand, general picture of the reaction environment in the sonoreactor has been determined with the information obtained by different methods:

- Aluminium and numerical methods present a mainly active zone just along the axial direction, located at the emitter centre($|X|<20$ mm) at X=0. Outer volume $X>\pm 20$ mm does not present erosion action in the aluminium test or high values of pressure amplitude.

- A gradual decrease in the ultrasonic field activity with the distance from the emitter is obtained by thermal and numerical simulation. This situation is roughly confirmed by aluminium test. A local maximum is located at 2.5 cm.
- The implementation of additional tools in the sonoreactor changes the configuration of the ultrasonic field. This information is very important in order to achieve reproducibility in further experiments.

Further work is planning for the implementation of a more complex numerical methods which consider the cavitation events and also the systematic characterization of higher frequency sonoreactors (300 kHz).

Acknowledgements

The authors would like to thank Universidad de Alicante for financial support under project GR03-05.

References

[1] T. J. Mason Ultrason. Sonochem. 10 (2003) 175-179.

[2] 4th Conference in Applications of Power Ultrasound in Physical and Chemical Processing, Bresançson, France, May 2003.

[3] P. R. Gogate, I. Z. Shirgaonkar, M. Sivakumar, P. Senthilkumar, N. P. Vichare, A. B. Pandit AIChE J. 47 (2001) 2526-2538

[4] P. R. Gogate, S. Mujumdar, A. B. Pandit, Adv. Env. Res. 7 (2003) 383

[5] P. G. Kanthale, P. R. Gogate, A. B. Pandit, A. M. Wilhelm, Ultrason. Sonochem. 10 (2003) 331-335.

[6] V. S. Moholkar, S. P. Sable, A. B. Pandit AIChE J. 46 (2000) 684-694

[7] M. Chanon, J.-L. Luche, Sonochemistry: Quo Vadis, in: J.-L. Luche (Ed.), Synthetic Organic Chemistry, Plenum 1998, pp. 376-392.

[8] E. A. Neppiras, IEEE Trans. on Sonics and Ultrasonics 2 (1968) 81

[9] J. K. Zieniuk, R. C. Chivers Ultrasonics 14 (1976) 161

[10] T. J. Mason, J. P. Lorimer, Sonochemistry, Theory, Applications and Uses of Ultrasound in Chemistry Ellis Horwood Ltd., 1998

[11] K. S. Suslick Ultrasound, its Chemical, Physical and Biological Effects, VCH, 1988.

[12] B. Pugin Ultrasonics 25 (1989) 49-55.

[13] M. M. Chivate, A.B. Pandit. Ultrason. Sonochem. 2 (1995) 19-25.

[14] D. Krefting, R. Mettin, W. Lauterborn, 4th Conference in Applications of Power Ultrasound in Physical and Chemical Processing, Bresançson, France, May 2003. p. 19-22

[15] C.J. Martin, A.N.R. Law. Ultrasonics 21 (1983) 85-90.

[16] C.J. Martin, A.N.R. Law. Ultrasonics Mayo (1980) 127-133.

[17] M. Romdhane, C. Gourdon, G. Casamatta, Ultrasonics 33 (1995) 221.

[18] M. Romdhane, C. Gourdon, G. Casamatta, Ultrasonics 33 (1995) 139.

[19] F. Faïd, M. Romdhane, C. Gourdon, A. M. Wilhelm, H. Delmas Ultrason. Sonochem. 5 (1998) 63-68.

[20] F. R. Contamine, A. M. Wilhem, J. Berlan, H. Delmas, Ultrason. Sonochem. 2 (1995) 43-47.

[21] M. A. Margulis, A. N. Mal'tsev, Russ. J. Phys. Chem. 43 (1969) 592-595

[22] T. J. Mason, Practical Sonochemistry: User's Guide to Aplications in Chemistry and Chemical Engineering Ellis Horwood, West Sussex, 1991, p. 43-46.

[23] T. Kimura, T. Sakamoto, J.-M. Leveque, H. Somiya, M. Fujita, S. Ikeda, T. Ando, Ultrason. Sonochem. 3 (1996) 157-161.

[24] J. P. Lorimer, T. J. Mason, K. Fiddy, Ultrasonics 21 (1991) 338.

[25] M. A. Margulis, I. M. Margulis, Ultrason. Sonochem. 10 (2003) 343-345.

[26] J. –L. Laborde, C. Bouyer, J. –P- Caltagirone, A. Gérard, Ultrasonics 36 (1998) 581-586

[27] M. Chouvellon, A. Largillier, T. Forunel, P. Boldo, Y. Gonthier, Ultrason. Sonochem. 7 (2000) 207-211

[28] G. Servant, J. P. Galtagirone, A. Gérard, J. L. Laborde, A. Hita Ultrason. Sonochem. 7 (2000) 217-277.

[29] J. L. Laborde, A. Hita, J. P. Galtagirone, A. Gérard Ultrasonics 38 (2000) 297-300

[30] A. Gachagan, D. Speirs, A. McNab Ultrasonics 41 (2003) 283-288.

[31] P. Boldo, V. Renaudin, N. Gondrexon, M. Chouvellon, Ultrason. Sonochem. 11 (2004) 27-32.

[32] F. Ihlenburg, Finite Element Analysis of Acoustic Scattering. Springer-Verlag, 1998

[33] F. Ihlenburg and I Babuška, Comput. Math. Appl., 30(9): 9-37, 1995

[34] F. Ihlenburg and I Babuška, SIAM J. Numer. Anal., 34(1):315-358, 1997

[35] I. Harari, TJR Hughes, Comput. Method Appl. M., 87:59-96, 1991

[36] I Babuška, F. Ihlenburg, T. Strouboulis, SK. Gangaraj, Int. J. Numer. Meth. Eng., 40:3443-3462, 1997

[37] I Babuška, F. Ihlenburg, ET. Paik, SA. Sauter, Comput. Method Appl. M., 128:325-359, 1995

[38] F. Ihlenburg and I Babuška, Int. J. Numet. Meth. Eng., 38:3745-3774, 1995

[39] I Babuška, T. Strouboulis, CS. Upadhyay, SK. Gangaraj., 38:4207-4235, 1995

[40] I Babuška, F. Ihlenburg, T. Strouboulis, SK. Gangaraj, Int. J. Numer. Meth. Eng., 40:3883-3900

[41] A. Deraemaeker, I Babuška,, P. Bouillard, Int. J. Numer. Meth. Eng., 46:471-499, 1999

[42] K. Gerdes, F. Ihlenburg, Comput. Method Appl. M., 170:155-172, 1999

[43] A. Moussatov, C. Granger, B. Dubus, Ultrason. Sonochem. 10 (2003) 191-195.

Figure captions

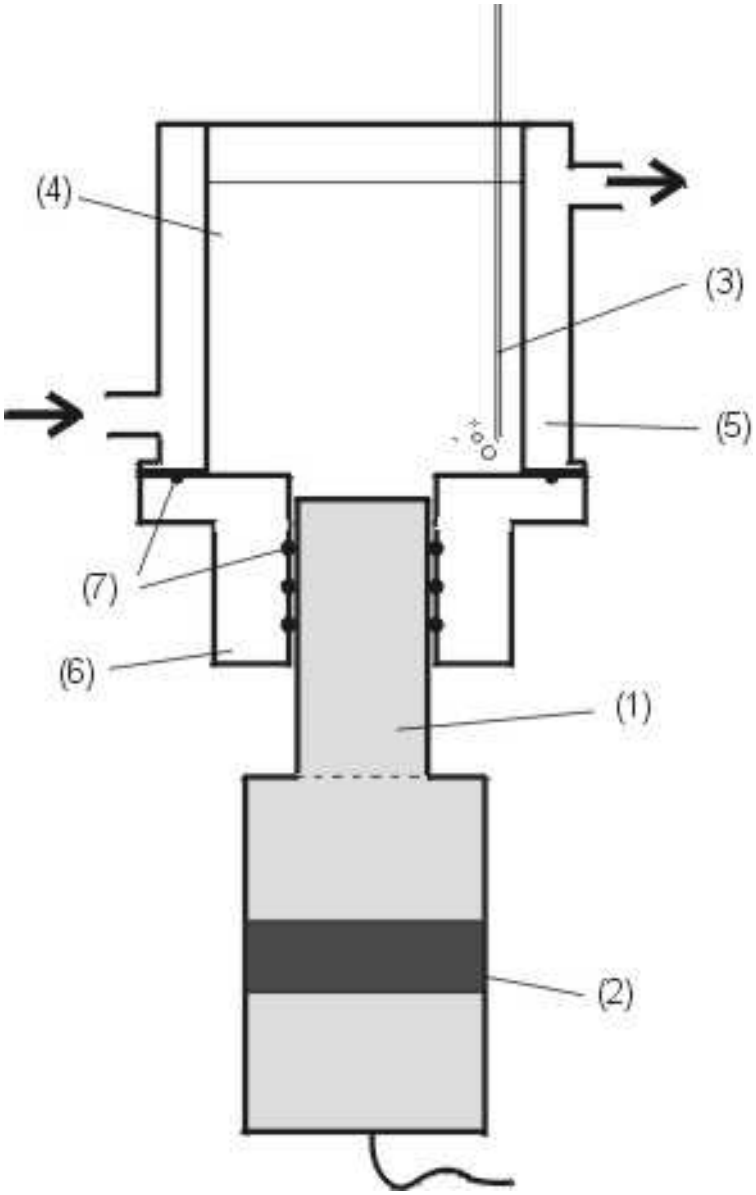

Figure 1.- Diagram of the experimental set-up: (1) ultrasonic probe, (2) transductor, (3) gas passing, (4) water, (5) cooling jacket, (6) Teflon adapter, (7) O-ring joints.

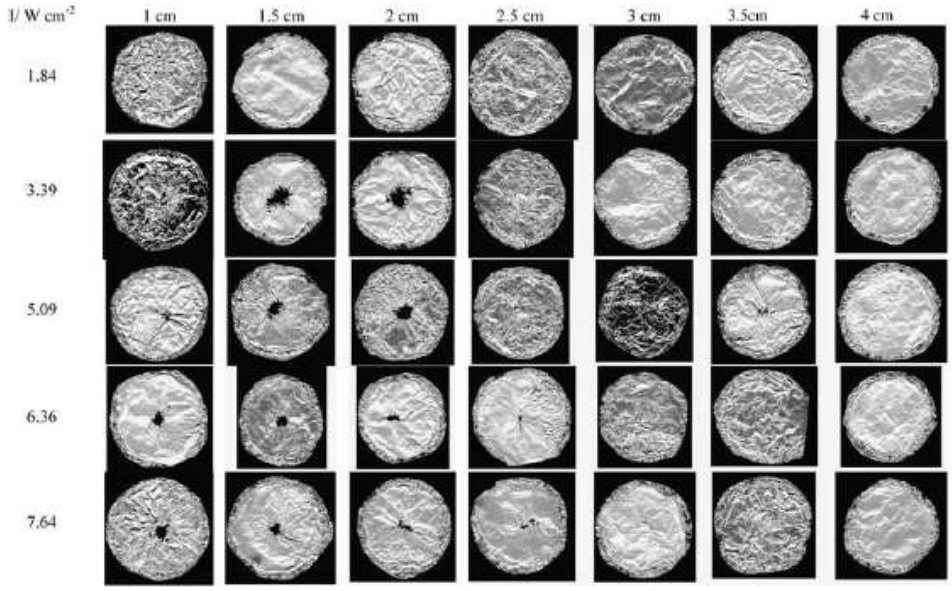

Figure 2.- Effect of the ultrasound intensity on the erosion of an aluminium foil (exposure time 40 s) placed parallel to the emitter surface at different global ultrasonic intensities (1.84, 3.39, 5.09, 6.36 and 7.64 W cm^{-2}) and foil-emitter surface distances (1, 1.5, 2, 2.5, 3, 3.5 and 4 cm).

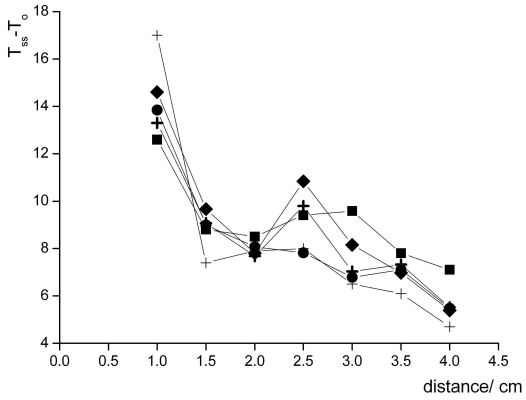

Figure 3.- (Local) Ultrasonic intensity profile for different global ultrasonic intensities (+) 1.84, (■) 3.39, (●) 5.09, (◆) 6.36, (✚) 7.64 W cm^{-2}.

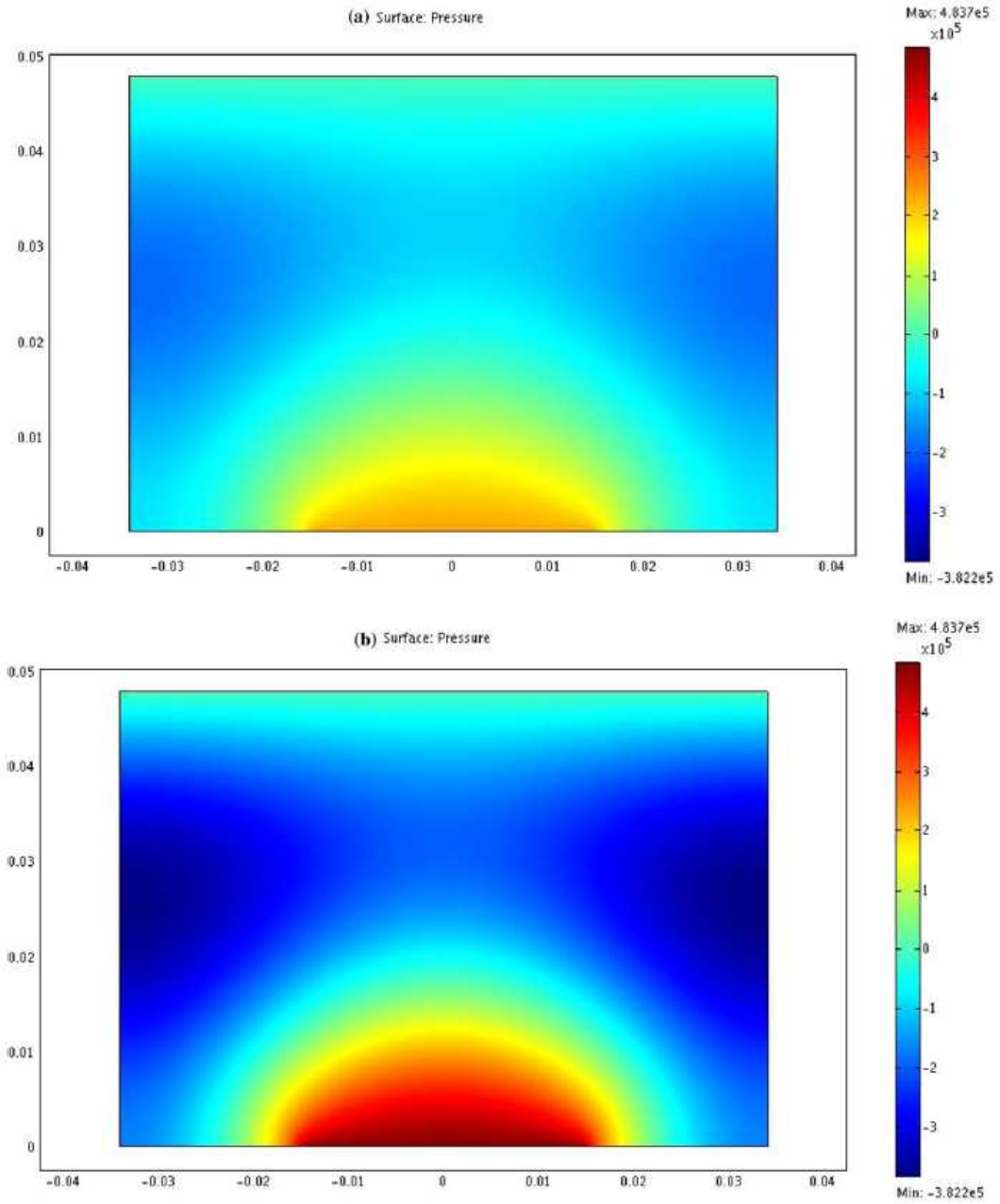

Figure 4. Spatial variations in pressure amplitude for a circular plane piston transducer with a radius=15mm, working at 20 kHz (a) global ultrasonic intensity 1.84 W cm^{-2} (b) 7.64 W cm^{-2}.

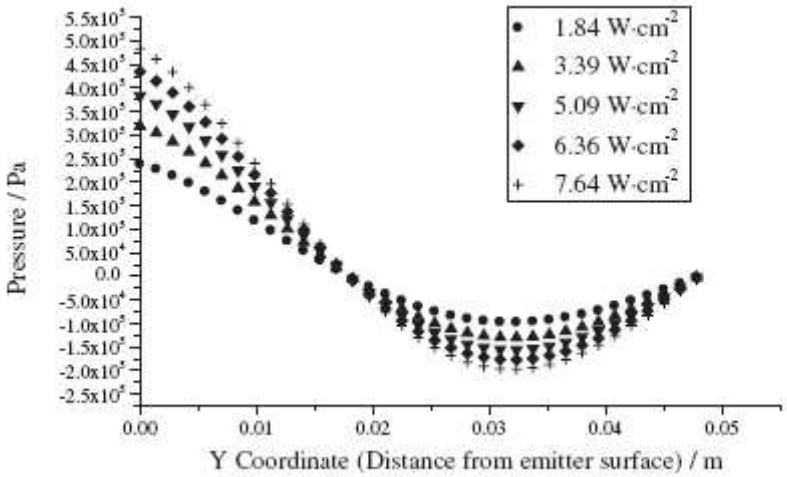

Figure 5.- Pressure profile in the axial direction at the centre of the surface emitter for different global ultrasonic intensities.

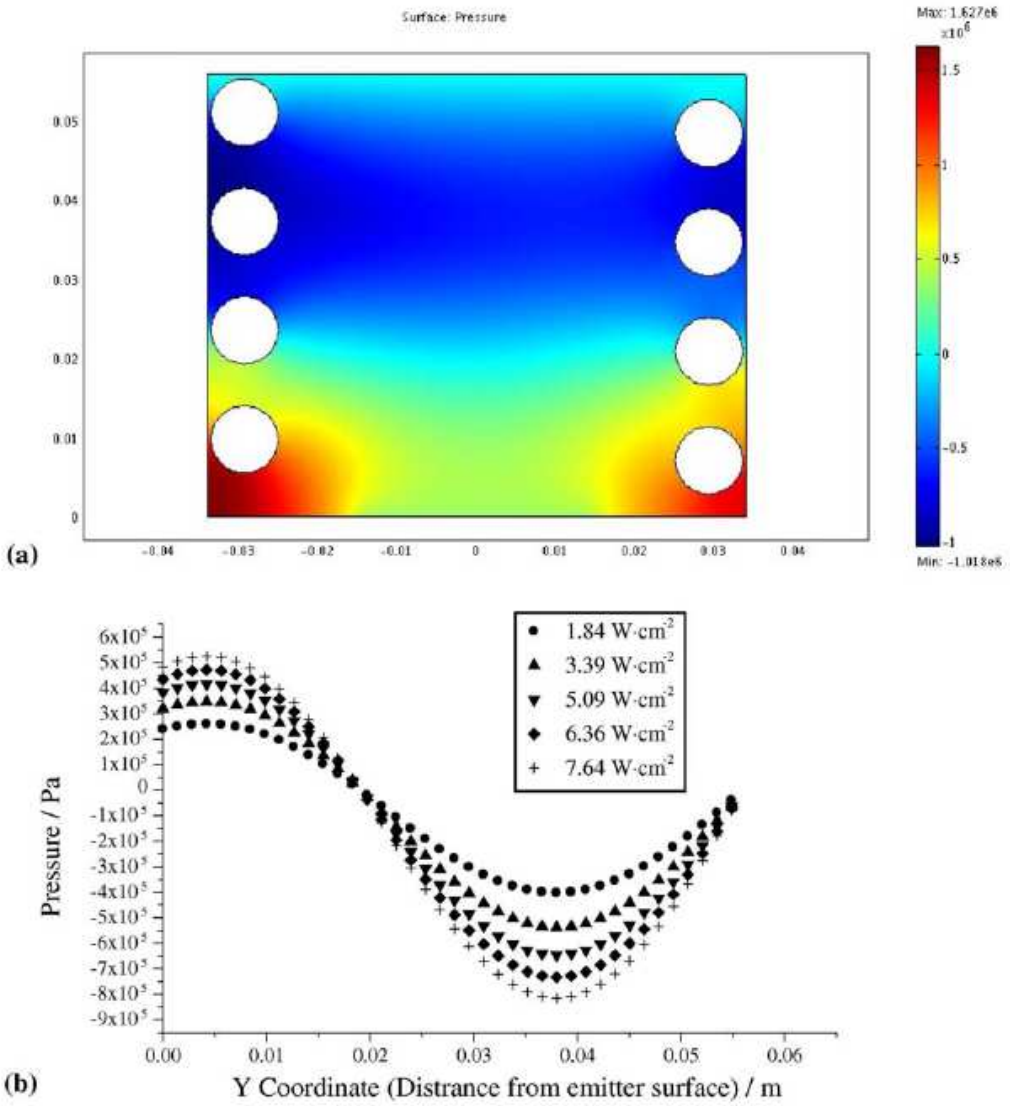

Figure 6. Influence of the glass cooling coil on ultrasonic field at a global ultrasonic intensity of 5.09 W cm^{-2} in (a) the spatial variations of the pressure amplitude, (b) the pressure profile in the axial direction at the centre of the surface emitter.

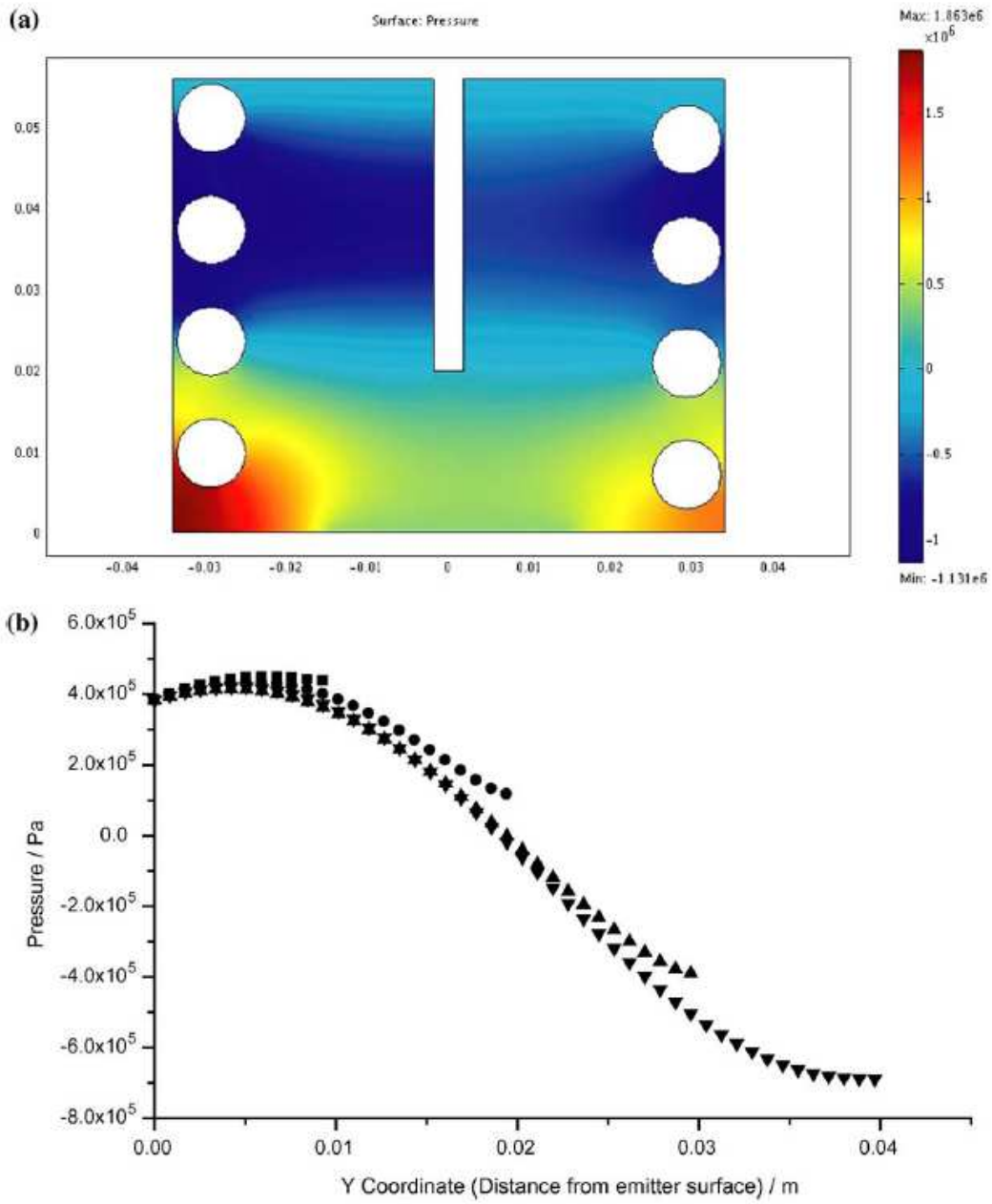

Figure 7. Influence of a rod on the ultrasonic field at a global ultrasonic intensity of 5.09 W cm^{-2} in (a) the spatial variations of the pressure amplitude, (b) the pressure profile in the axial direction at the centre of the surface emitter.